TRANSITION OF WAVE PACKETS ORIGINATING FROM LOCALIZED STRONG DISTURBANCES IN LAMINAR BOUNDARY-LAYER OF ROTATING-DISK FLOW

Akira Nishizawa
Fluid Science Research Center, NAL (JST)
7-44-1 Jindaiji-higashimachi, Chofu, Tokyo 182-8522, Japan
kei@nal.go.jp

Shohei Takagi
Fluid Science Research Center, NAL
pantaka@nal.go.jp

Naoko Tokugawa
Fluid Science Research Center, NAL
nao@nal.go.jp

ABSTRACT
A laminar to turbulent transition process for a three-dimensional boundary layer in a rotating-disk flow initiated by localized disturbances was experimentally investigated. The hot-wire analysis showed that the point disturbance develops into a turbulent patch. The turbulent patch propagating in the wedge region is accompanied by two families of traveling waves, which consist of the so-called cross-flow and streamline-curvature modes. The configuration in the plane view of the turbulent patch is a crescent, which is different from an arrowhead-shaped turbulent spot in a Blasius boundary layer.

INTRODUCTION
It is well known that strong localized disturbances initiate turbulent spots in two-dimensional laminar boundary layers (Schubauer & Klebanoff, 1955). For three-dimensional boundary layers, no attention has been paid to the behavior of such strong localized disturbance although the stationary longitudinal vortices due to cross-flow instability have been generally observed (Gray, 1952; Gregory et al., 1955). Lingwood(1996) studied the development of a weak localized disturbance in a rotating-disk flow, typifying a three-dimensional laminar boundary layer. She revealed that such a disturbance grows into a wave packet which consists of two types of waves, but did not trace the wave behavior all the way to turbulent breakdown. The present experiment mainly focuses on the breakdown to turbulence of the strongly introduced disturbance and development of the turbulence region in the rotating-disk flow.

Another interesting feature of such a localized turbulent structure is its boundary region because it is known that the fully developed turbulent spot in a two-dimensional boundary layer is accompanied by oblique wave packets (Wygnanski et al., 1979) due to a Tollmien-Schlichting instability at its trailing edge. In cases of three-dimensional boundary layers, there are two different kinds of instability, namely cross-flow (hereinafter referred to as C-F) instability and streamline-curvature (S-C) instability (Itoh, 1994; 1998a). Takagi et al. (1999) experimentally investigated the unstable disturbances generated by continuous forcing through a point source in a rotating-disk flow and showed for the first time the separated appearance of the two traveling modes resulting in good agreement with the linear stability theory by Itoh (1998a,b). In the present investigation, the characteristic features of two types of traveling waves around the localized turbulent region originating from the strong disturbance are also discussed in comparison with Itoh's linear stability theory.

EXPERIMENTAL APPARATUS
Figure 1 shows a schematic of the experimental set up. A round aluminum disk with a diameter of 800 mm was horizontally placed in a still fluid. A small hole with an inner diameter of 0.5mm was drilled at r=190mm to introduce a pulsed jet by a small speaker installed underneath the hole. Maximum velocity of the jet measured in the still fluid is V_{jmax}=6.9m/s and the duration is about 7ms as shown in Fig.2. The disk rotates at Ω=4.4[rps] in the counter-clockwise direction on a vertical hollow shaft, at whose end a low-noise rotary connector for the speaker was attached. The Reynolds number $R=r(\omega_D/\nu)^{1/2}$ is about 256 at the hole which is slightly sub critical to the C-F instability predicted by linear stability theory (Itoh, 1996), where $\omega_D=2\pi\Omega$ [rad/s] is the angular velocity and ν is the kinematic viscosity. A photo sensor generated a reference signal for every rotation of the disk but the pulsed jet was introduced for every two rotations to avoid the superposition of disturbances. A conditional sampling with a hot-wire probe was done

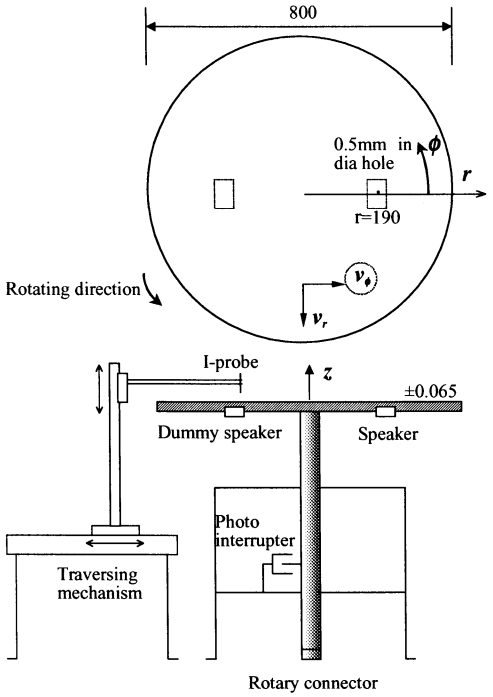

Figure 1. Schematic of experimental setup. Unit: mm

in a laboratory fixed reference frame. The wire of the I-probe was placed parallel to the radial direction and the disk surface to measure the circumferential velocity component. All results presented here were obtained at z=1.0mm ($\zeta=z(\omega_D/\nu)^{1/2}\approx1.35$). The origins of the radial, circumferential and vertical axes are located at the center of the disk, the hole and the surface, respectively. Time t is normalized by the rotation cycle T. The delay time, t_D, from the reference signal to a rising edge of the speaker driving pulse defined by t=0 was changed between t_D=0 and t_D=0.97T at intervals of 0.022T (corresponding to 7.92°) such that the hot-wire probe passes through various locations in the wave packets at the same radius. The 4096-point data (1.8T) was collected by analogue-to-digital converter at a sampling rate of 10kHz. The calculations of the ensemble-averaged circumferential velocity, $\langle v\rangle$, and ensemble-averaged turbulence intensity, $\langle v'\rangle$, are as follows,

$$\langle v(\phi,t)\rangle=\frac{1}{N}\sum_{i=1}^{N}v_i(\phi,t) \qquad (1)$$

$$\langle v'(\phi,t)\rangle=\sqrt{\frac{1}{N}\sum_{i=1}^{N}\left(v_i(\phi,t)-\langle v(\phi,t)\rangle\right)^2} \qquad (2)$$

where v_i is the fluctuating circumferential velocity of the ith realization at certain time t and angle ϕ normalized by the local disk speed and N =64 is the number of total realizations.

RESULTS AND DISCUSSION

Effect of initial condition

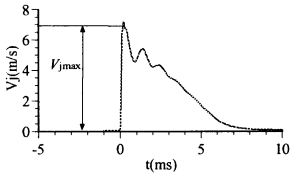

Figure 2. Waveform of a pulsed jet measured at r=190mm and z=1mm without the disk rotation.

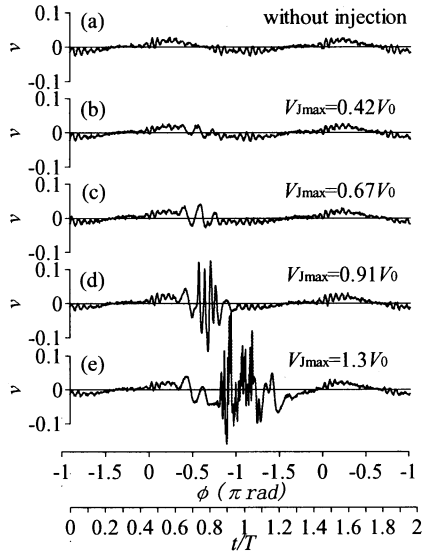

Figure 3. Instantaneous waveforms of the velocity fluctuation v at R=450 for various strength of the pulsed jet. V_0 is the local disk speed at the disturbance source.

Aspects of the disturbances drastically change depending on their initial condition. Figure 3 illustrates instantaneous waveforms observed at R=450 for various strength of the pulsed jets. The initial condition of the artificial disturbance was selected as follows. The weaker disturbance develops into a wave packet (Fig.3b) and the increase in the strength of the jet brings about the well-developed wave packet (Fig.3c). Further increase in the strength causes a packet having shorter wavelength (Fig.3d) and eventually the disturbance breaks down into turbulence (Fig.3e). The present experiment was conducted under the condition of the strongest disturbance as shown in Fig.3e to observe the well developed localized turbulent structure in the rotating-disk flow.

Localized turbulent patch

Figure 3e shows that the turbulence coexists in the presence of unstable waves in the boundary layer. Since such coexistence makes it difficult to strictly distinguish the turbulent region from laminar region, an ensemble average technique is applied to observe the configuration of turbulent region. Figure 4 shows contour maps of the ensemble-averaged turbulence intensity in the r-ϕ plane at six different times. The boundary between the turbulent and

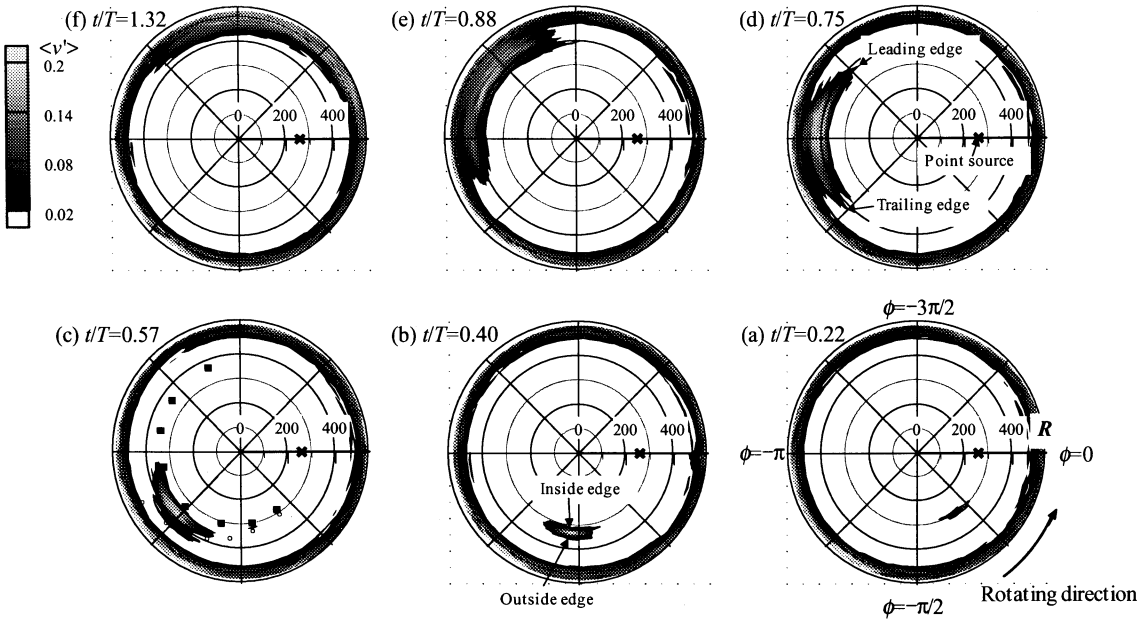

Figure 4. Contour maps of ensemble-averaged turbulence intensity <v'> at various instances. Open circles and closed squares in (c) indicate the propagation region of the disturbance.

laminar states presented here is defined as the envelope of contours for which <v'>≥0.02. For all of the figures, there are naturally occurring turbulent regions at R≥500 due to the development of stationary vortices. An isolated small turbulent patch can be observed at t/T=0.22 and at R≈300 (Fig.4a). This patch grows with the passage of the time and moves opposite to the rotation direction. In excess of the line of R=300, the circumferential length scale of the patch in Fig.4b is observed to approximately double, compared with Fig.4a. Although not shown, such a turbulent patch is not observed at t/T<0.15 but it appears at R≈280 which is close to the critical Reynolds number for C-F instability. The shape of the turbulence region is approximately crescent, in contrast with the arrowhead-shaped turbulent spots (Schubauer & Klebanoff, 1955) in a Blasius boundary layer and is similarly kept in the downstream direction. As shown in Fig.4c, the trajectory of the propagation plotted by open circles and solid squares indicates that the localized disturbance expands in a wedge-like region but it never moves inward. Since the patch keeps growing downstream, a part of the patch is still retained on the disk even after one cycle of the rotation as shown in Fig.4f.

In order to clarify the characteristic features in propagation of the turbulent patch, the trajectories of its edges are plotted in Fig. 5. The tips of the turbulence region in the circumferential direction are defined as leading and trailing edges while the tips in the radial direction are defined as inside and outside edges. Figure 5a shows that both leading and trailing edges propagate outboard proportional to time. The calculated convection velocities of leading and trailing edges are $0.85\omega_D$ and $0.47\omega_D$, respectively. Schubauer & Klebanoff (1955) showed that the leading and trailing edges of the turbulent spot in a two-dimensional boundary layer are convected at a speed of $0.88U_\infty$ and $0.5U_\infty$, respectively. These values are found to be similar to those of the present result. Matsui (1980) clarified that the turbulent spot is an assemblage of the small-scale hairpin or longitudinal vortices and the generation of the new vortices at the trailing edge gives birth to a difference between convection velocities of the leading and trailing edges. Although Perry (1981) suggested a different model, namely the generation of new vortices at the leading edge causes streamwise growth of the spot, it is prevailingly recognized till now that new vortices are mainly produced at the trailing edge (Sankaran et .al, 1988). Considering the results observed by Matsui, there is a possibility that the turbulent patch in the rotating-disk boundary layer grows in the circumferential direction due to successive generation of new vortices at the edge. However, it is difficult to draw a conclusion as to which edge of the turbulent patch contributes to generate new-vortex system. This is because the ensemble-averaged contour maps of the turbulent region illustrated in Fig.4 do not show structural evidence of any vortices. Another measurement techniques are necessary to separate coherent structures associated with vortex motion from random fluctuations superimposed on individual structures in the turbulent region; e.g. multiple-hotwire

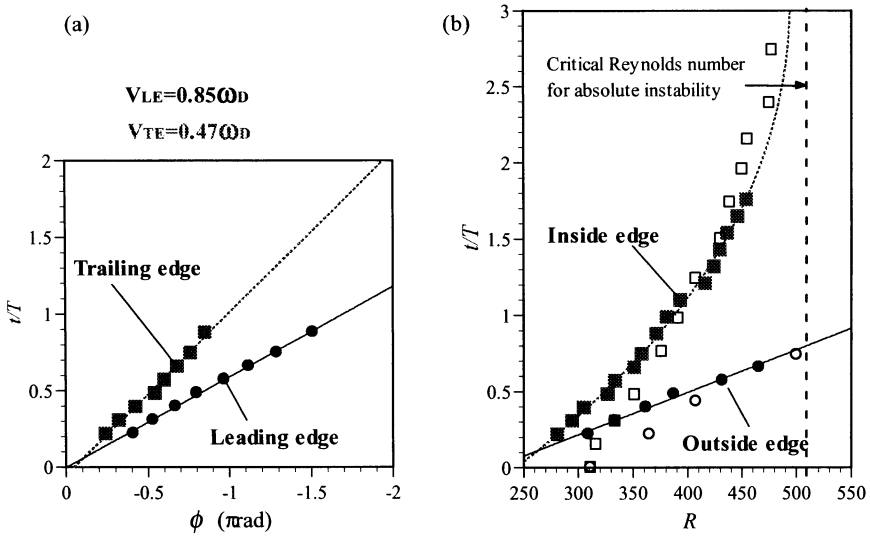

Figure 5. Propagation of the turbulent patch. (a) Trajectories of leading and trailing edges in the circumferential direction. (b) Trajectories of outside and inside edges in the radial direction. Solid symbols indicate the present results. Open symbols in (b) are the result by Lingwood (1996) for the wave packet originating from a localized weak disturbance.

measurements by Makita and Nishizawa (2000) for internal structures of turbulent spots.

Fig.5b shows the trajectories of outside and inside edges in the radial direction. In general, a three-dimensional boundary layer flow can become unstable to a convective instability but Lingwood (1996) suggested the possibility of another instability mechanism, namely an absolute instability; a group velocity of the disturbance tends to zero but it develops with reference to time. The tendency of the trajectory of inside edge to zero-gradient is known to be an important feature for the occurrence of the absolute instability. The results by Lingwood for the wave packet originating from a weak localized disturbance are superimposed on the same figure. It is found that the inside edge does not convect proportional to time. Furthermore, in spite of the fact that the magnitude of the initial disturbance and the Reynolds number at the forcing point are different between the present and her experiment, both results seem to tend toward the same final state. However, whether the coincidence is due to the absolute instability or the other mechanism remains inconclusive. This is the reason why it is impossible to keep track of the turbulent patch because it enters into the regime of naturally growing cross-flow vortices fixed relative to the disk before it achieving at the critical Reynolds number of the absolute instability suggested by Lingwood. Similar difficulty was reported by Bippes (1999) who experimentally studied the instability of a swept wing boundary layer by means of a water towing tank. More detailed experiments are required to discuss the relation between the propagation of the turbulent patch and absolute instability.

Instability waves around the turbulent patch

Figure 6a shows the instantaneous waveforms of velocity fluctuation v corresponding to the incipient wave packet at R=270. Note that the abscissa is taken in reverse form used in Fig.3 to permit ready comparison with the contour maps in Fig4. The repeatability of the waveforms is good (not shown here) and no breakdown is observed at this location. The incipient wave packet seems to be composed of only one type of wave. A breakdown can be observed in the wave packet at R=300 and t_D/T=0.44 as shown in Fig.6b. On the other hand, no breakdown is observed at the other delay time t_D shown in the top and bottom traces, indicating that the transition to turbulence begins to occur in the middle of the wave packet and the resultant turbulent region is accompanied by laminar-like waves at its periphery.

Figures 6c and 6d show the instantaneous waveforms of velocity fluctuation at R=350 and 450, respectively. It should be noted that these waveforms give quite different impression with variation of the delay time t_D because the disturbance grows larger and passes through the measuring line of the hot wire during the rotation. For all of the waveforms, the same position on the abscissa corresponds to the same time while the angular position differs with each delay time. For R=350, three typical waveforms roughly show that one traveling wave having longer wavelength in circumferential direction appears prior to the turbulent-like spikes following the third wave with comparatively shorter wavelength. The randomization in the turbulent patch progresses with increase of Reynolds number as shown in the middle trace of Fig.6d. Two types of waves having different wavelengths are also observed in top and bottom

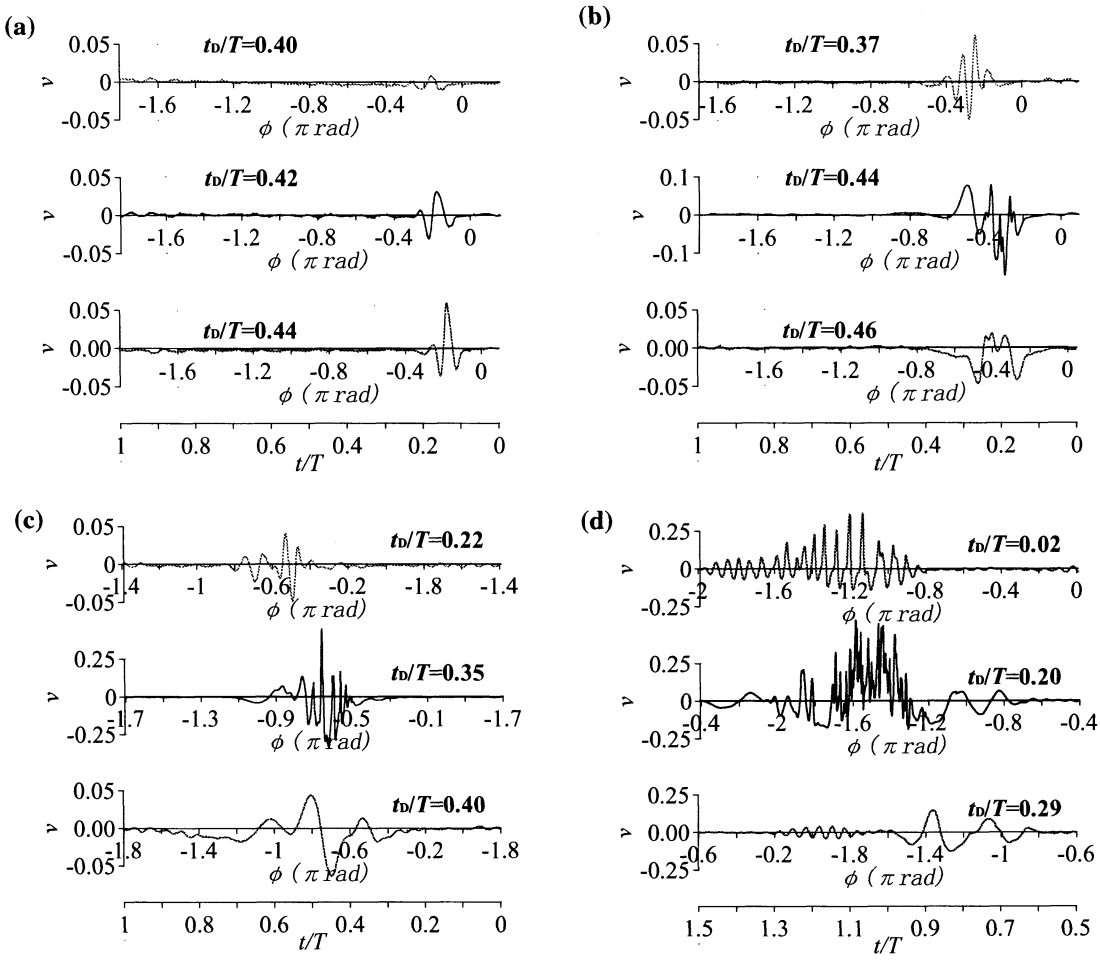

Figure 6. Instantaneous waveforms of velocity fluctuation v at various Reynolds numbers. (a) R=270, (b) R=300, (c) R=350, (d) R=450.

traces in this figure. These facts reveal that the turbulent patch in the rotating-disk flow grows with two different types of waves around it. Apparently, it is difficult to quantitatively determine the wavelength and frequency of these waves only from Fig.6 because the time and angular position on these waveforms simultaneously change with rotation of the disk. For turbulent spots, it is known that two oblique Tollmien-Schlihting wave packets attach to the trailing edge (Wygnanski et al., 1979), but the growth of the spot is due to a different mechanism from T-S instability. In the present case, the following questions spring out: (1) Which is the dominant instability mechanism to cause the breakdown of the wave packet? ; (2) Is the breakdown of the waves around the turbulence region the main cause of the growth of the turbulent patch? ; (3) Is there another instability mechanism responsible for the growth? The answers however remain elusive. In order to identify the types of waves around the turbulent patch, the following figure showing the characteristic features of the waves is compared with linear stability theory by Itoh (1998b).

Figure 7 shows the contour of ensemble-averaged velocity fluctuation <v> in the ϕ-t plane at R=350. In the figure, the frequency of the velocity fluctuation can be evaluated because only time varies on a given

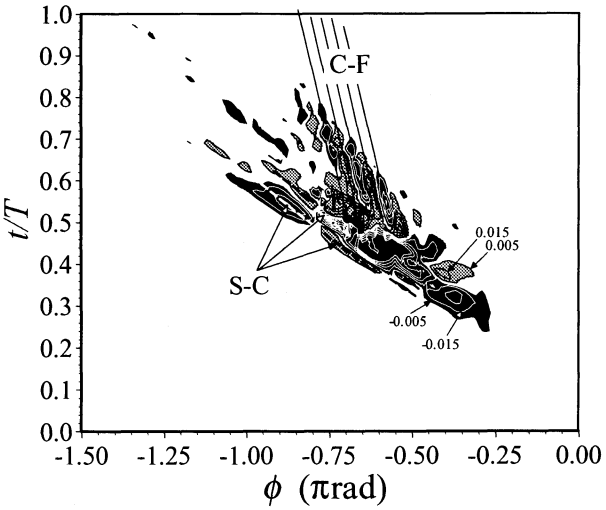

Figure 7. Contour of ensemble-averaged velocity fluctuation <v> in the ϕ-t plane at R=350. Solid and broken lines indicate wave crests. Gray and black regions indicate <v>>0 and <v><0, respectively.

line parallel to the vertical axis. It is clearly observed that the disturbance forms a wave packet accompanied by two types of waves denoted by solid and broken lines. The fact that these lines incline to the time axis documents that they consist of traveling waves. For the solid lines, the normalized frequency and wave number in ϕ-direction are estimated as $\hat{\omega} \approx 5$ ($f \approx 22$Hz) and $n \approx 32$, respectively, where $\hat{\omega}$ is defined by $\hat{\omega} = 2\pi f/\omega_D$. These values are in good agreement with the theoretical prediction by Itoh(1998b, Fig.2) ; $\hat{\omega} = 4.0$ ($f = 17.6$Hz) and $n \approx 33$, for the most unstable C-F mode at $R = 350$, although his calculation was carried out for unstable disturbances generated by continuous forcing through a pinhole. For the broken lines in Fig.7, the estimated frequency is $\hat{\omega} \approx 12.5$ ($f \approx 55$Hz) which also agrees well with results by Itoh (1998b); $\hat{\omega} = 15$ ($f = 66$Hz) for the most unstable S-C mode. As indicated, two types of waves around the turbulent patch are clearly identified; namely, C-F and S-C traveling modes. For a more detailed analysis and understanding about the role of these instability modes on the growth of the turbulent patch, additional measurements with much higher spatial resolution are required.

CONCLUDING REMARKS

(1) A localized strong disturbance originating from a point source develops into a wave packet and its velocity fluctuation is spatially amplified in a three-dimensional laminar boundary layer on a rotating-disk.

(2) As the wave packet grows downstream, the breakdown to turbulence occurs in the middle of the packet and results in the formation of a turbulent patch.

(3) The turbulent patch propagating in the wedge region is accompanied by the two families of traveling waves composed of the so-called cross-flow and streamline-curvature modes.

(4) The configuration in the plane view of the turbulent patch is a crescent, which is different from an arrowhead-shaped turbulent spot in a Blasius boundary layer.

(5) The leading and trailing edges of the turbulent patch convect in the circumferential direction at 0.85 and 0.47 local disk speeds, respectively.

Acknowledgements

The authors wish to express their appreciation to Dr.Itoh,N. National Aerospace Laboratory for his helpful discussion and advice. The authors' appreciation extends to Professor Buck, G. A., South Dakota School of Mines and Technology, who gave suggestive comments during his stay at NAL, which partly initiated the present study. The authors are also grateful to him for kindly correcting the text.

References

Bippes, H., 1999, "Basic experiments on transition in three-dimensional boundary layers dominated by crossflow instability", *Progress in Aerospace Sci.*, vol.35, pp. 363-412.

Gray ,W.E., 1952, "The nature of the boundary layer flow at the nose of a swept wing", RAE TM Aero, 256.

Gregory, N., Stuart,J.T. & Walker,W.S., 1955, "On the stability of three-dimensional boundary layers with application to the flow due to a rotating disk", *Phil. Trans. R. Soc. London A*, vol.248, pp. 155-199.

Itoh, N., 1994, "Instability of three-dimensional boundary layers due to streamline curvature", *Fluid Dyn. Res.*, vol.14, pp. 353-366.

Itoh, N., 1996, "Simple cases of the streamline-curvature instability in three-dimensional boundary layers", *J. Fluid Mech.*, vol.317, pp. 129-154.

Itoh, N., 1998a, "Theoretical description of instability waves in the flow on rotating disk - Part 1. False-expansion method applied to linear stability equations", *Trans. Japan Soc. Aero. Space Sci.*, vol.40, pp. 262-279.

Itoh, N., 1998b, "Theoretical description of instability waves in the flow on rotating disk - Part 2. Development of wedge-shaped disturbances", *Trans. Japan Soc. Aero. Space Sci.*, vol.40, pp. 280-292.

Lingwood, R.J., 1996, "An experimental study of absolute instability of the rotating-disk boundary-layer flow", *J. Fluid Mech.*, vol. 314, pp. 373-405.

Matsui, T., 1980, "Visualization of turbulent spots in the boundary layer along a flat plate in a water flow", *Laminar-Turbulent Transition* in IUTAM Symp., R. Eppler and H. Fasel, ed., Springer-Verlag, pp. 288-296.

Makita, H. & Nishizawa, A., 2000, " Characteristics of Internal Vortical Structures in a Merged Turbulent Spot." *8th European Turbulence Conference EUROMECH*, pp. 337-340.

Perry, A.E., Lim, T.T. & Teh, E.W., 1981, "A visual study of turbulent spots", *J. Fluid Mech.*, vol.104, pp. 387-405.

Sankaran, R., Sokolov, M. & Antonia, R.A., 1988, "Substructures in a turbulent spot", *J. Fluid Mech.*, vol.197, pp. 389-414.

Schubauer, G.B. & Klebanoff, P.S., 1955, "Contributions on the mechanics of boundary-layer transition", N.A.C.A. TN 3489, pp. 1-31.

Takagi, S., Tokugawa, N., Itoh, N. & Nishizawa, A., 1999, "Characteristic features of traveling disturbances originating from a point source in rotating-disk flow", *Laminar-Turbulent Transition* in IUTAM Symp., H.F. Fasel and W.S. Saric, ed., Springer-Verlag, pp. 637-642.

Wygnanski, I., Haritonidis, J.H. & Kaplan, R.E., 1979, "On a Tollmien-Schlichting wave packet produced by a turbulent spot", *J. Fluid Mech.*, vol.92, pp. 505-528.